ELSEVIER

Polymer 42 (2001) 3847–3858

polymer

www.elsevier.nl/locate/polymer

Toughening of a trifunctional epoxy system Part VI. Structure property relationships of the thermoplastic toughened system

R.J. Varley[a,*], J.H. Hodgkin[a], G.P. Simon[b]

[a]*CSIRO Molecular Science, Bayview Avenue, Clayton, Vic. 3168, Australia*
[b]*Department of Materials Engineering, Monash University, Clayton, Vic. 3168, Australia*

Received 4 May 1999; received in revised form 18 April 2000; accepted 13 June 2000

Abstract

This paper examines the effect of the addition of PSF upon the final properties and network structure of the TGAP/DDS system after cure and post-cure. It also compares the differences in the network structure and properties of the modified system between samples in which the epoxy resin and thermoplastic had been prereacted and those which had been simply mixed together. The thermal properties of the network structure were investigated using dynamic mechanical thermal analysis while the chemical structures were characterised using near infra-red spectroscopy. Physical properties such as water uptake, density and mechanical properties such as toughness, modulus, compressive strength and yield stress were measured. © 2001 Elsevier Science Ltd. All rights reserved.

Keywords: Epoxy resin; Thermoplastic toughening; Network structure

1. Introduction

It is well known that epoxy resins cure to form highly crosslinked materials which are inherently brittle. This has limited their further proliferation into other applications which require more impact resistant or "tougher" materials. This drawback has prompted many studies devoted to increasing their fracture resistance without compromising their desirable attributes, such as their high glass transition temperature (T_g), high modulus and advantageous strength to weight ratios. The most common strategy employed has been to add a second "tough" phase, which is initially miscible in the epoxy resin but phase separates at some point during cure to form a thermoplastic rich phase and an epoxy rich phase. This produces a multiphase morphology which is able to initiate toughening mechanisms which can dissipate the energy of a propagating crack hence increasing toughness. The most common additives by far, to date have been carboxy terminated butadiene rubbers (CTBN), which are found to impart large increases in toughness particularly for the lower crosslinked epoxy resin systems. However, a disadvantage with rubber toughening agents is that they reduce desirable epoxy resin properties such as modulus and the glass transition temperature. For example, Sankaran and Chanda [1] found that the addition of 12% by weight of rubber caused the ultimate tensile strength and tensile modulus to decrease by 41 and 24%, respectively. They did, however, find that toughness of the resin system increased by 214%. For this reason, ductile engineering thermoplastics have been used as tougheners because they have high T_gs and moduli and thus do not compromise any of the desirable properties of epoxy resin systems. Early studies using thermoplastic toughening agents [2–4] were not particularly successful at increasing the fracture resistance of epoxy resins, but have prompted more studies which have investigated the effect on morphology, cure, thermoplastic endgroups and the chemical structure of the thermoplastic and epoxy resin. General criteria for thermoplastic toughening drawn from the literature are as follows:

1. *Thermoplastic backbone.* This must have good thermal stability, should be soluble in the uncured epoxy but must phase separate during cure to form a multiphase morphology [3–4].
2. *Morphology.* Optimum toughness increase is achieved through attainment of a co-continuous or phase inverted morphology [5–7].
3. *Reactive endgroups.* Their precise importance is unclear

* Corresponding author.
E-mail address: russell.varley@molsci.csiro.au (R.J. Varley).

0032-3861/01/$ - see front matter
PII: S0032-3861(00)00491-2

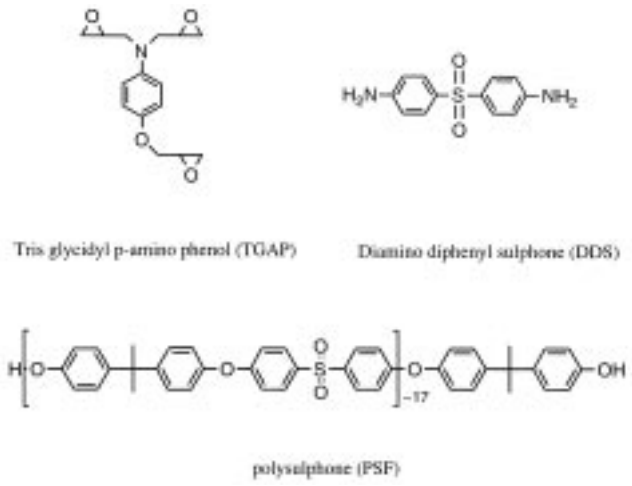

Fig. 1. Chemical structures of the materials used here.

from the literature, but appears to depend upon the thermoplastic used [8–13].

4. *Ductility of epoxy resin.* Thermoplastics toughen highly crosslinked materials more effectively than they toughen materials with a lower crosslink density [14–15].
5. *Molecular weight.* Increasing thermoplastic molecular weight has been shown to increase toughness [16–18], the ease of processing being the limiting factor.
6. *Cure.* The cure must be taken to completion to minimise unreacted functional groups, which introduce structural weaknesses [19–20].

This paper is the sixth in a series of studies, which has studied the effect of thermoplastic addition upon the cure and structure/property relationships of an epoxy resin system. This work presents an investigation of the network structure and the thermal, mechanical and physical properties of the cured and post-cured thermoplastic modified system. The paper also investigates the effect of initial "prereaction" between the TGAP and PSF upon the aforementioned properties.

2. Experimental

2.1. Epoxy resins and curing agent

The epoxy resin used in this study was tri-glycidyl *p*-amino phenol (TGAP; Ciba-Geigy), a tri-functional, low viscosity, amber liquid sold as Araldite MY0510. Prior to use, the resin was allowed to warm up to room temperature in sealed containers in order to prevent excessive moisture absorption. The curing agent or hardener used in all cases was 4,4′-diamino diphenyl sulphone (DDS; Ciba-Geigy), a pale pink powder sold as Araldite HT976. The thermoplastic modifier used in this study was a low molecular weight phenolic terminated bisphenol A polysulphone (PSF). It was synthesised from bisphenol A (Dow, $M_n = 228$ g/mol) and 4,4′-dichloro diphenyl sulphone (Aldrich, $M_n = 287$ g/mol) using a method described by Johnson et al. [21]. The final polysulphone was characterised via Fourier transform infrared spectroscopy (FT-IR), gel permeation chromatography (GPC) and differential scanning calorimetry (DSC). GPC determined the number average molecular weight to be 7800 g/mol, while nuclear magnetic resonance (NMR) analysis confirmed the molecular weight to be 8000 g/mol. The chemical structures of the epoxy resin, curing agent and thermoplastic modifier are shown in Fig. 1.

2.2. Sample preparation

A slightly off stoichiometric mixture of TGAP/DDS (1:0.9) of epoxide to amino groups, was used for all studies. The PSF modified resin mixtures were prepared via two different methods, which will be referred to as "prereacted" and "non-prereacted". The non-prereacted samples were prepared by mixing the PSF with the TGAP together on a rotary evaporator under vacuum at 130°C, until the PSF was completely dissolved and free of bubbles. The time that this took depended greatly on the amount of PSF added but was not longer than 30 min, even at the highest PSF concentration and largest sample size. Once dissolved, the DDS was added and mixing continued until the DDS had also completely dissolved and the mixture was free of bubbles. The "prereacted" samples were prepared by placing a methanolic solution of tetramethylammoniumhydroxide (TMAH) in a round-bottomed flask with the PSF and TGAP, which were both dissolved in a minimum quantity of dichloromethane. The solution was then mixed on the rotary evaporator under vacuum and heated to 130°C for 30 min to allow reaction between the TGAP and PSF to occur, as well as to completely remove the dichloromethane. The amount of TMAH used was kept constant at 1.6 w/w% of the amount of PSF used for each different formulation. The temperature was then increased to 165°C for a further 20 min in order to decompose any remaining TMAH. At this point the temperature was reduced to 130°C, DDS added and mixing continued until completely dissolved and free of bubbles.

Both prereacted and non-prereacted samples were prepared with 0, 10, 15, 20 and 30% (w/w) of PSF in the TGAP/DDS mixture. A 50% PSF non-prereacted mixture was also prepared. Each sample was poured into a relevant mould and cured in an air circulating oven at 150°C for 16 h. Half of each sample was then post-cured for 2 h at 205°C. For some of the measurements taken here, only post-cured samples were available for analysis.

2.3. Dynamic mechanical thermal analysis

The glass transition temperatures (T_g) of the cured samples were obtained from a Polymer Laboratories Mark II DMTA by clamping a rectangular bar with dimensions $10 \times 1.6 \times 45$ mm^3 in the dual cantilever bending mode with a 5 mm free length frame. The strain amplitude was set at 4 μm and the oscillating frequency used was 1 Hz as the

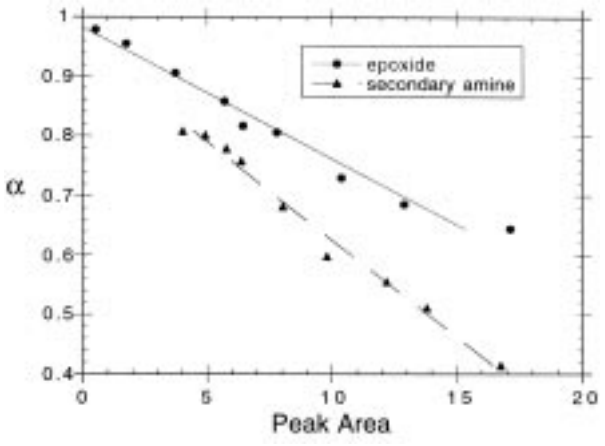

Fig. 2. Calibration curve of the calculated conversion for the epoxide (at 5881 cm^{-1}) and secondary amine (6577–6692 cm^{-1}) peaks after subtraction from the post-cured TGAP/DDS versus the absorbance areas.

temperature was scanned from 50 to 300°C at a constant heating rate of 2°C/min. The T_gs were measured from the peaks in the tan δ spectrum and used consistently as such throughout the work.

2.4. Near infra-red spectroscopy

Near infra-red (NIR) spectroscopy was performed on an Alpha Centauri FT-IR spectrophotometer (Mattson Instruments, USA) in the NIR mode. Spectra were recorded between 9000 and 4000 cm^{-1} using 32 scans at a resolution of 8 cm^{-1}. The theory and background to quantifying the epoxide and secondary amine conversions from the NIR spectra are described in a previous publication [22]. The difficulty with quantifying the PSF modified samples was that the NIR spectra of PSF contains an aromatic CH overtone peak which overlaps with the internal standard used previously [22]. This made it impractical to use the epoxide peak at 5881 cm^{-1} forcing the epoxide peak at 4522 cm^{-1} to be used. This was done by constructing a calibration curve, as shown in Fig. 2, using the results obtained from a similar study using cured neat resin samples [23]. The calibration curve consisted of the peak areas of both the epoxide and secondary amine groups at 4522 and 6577–6692 cm^{-1}, respectively, plotted versus the group conversions determined from the epoxide and secondary amine peaks at 5881 and 6577–6692 cm^{-1}. Using samples of equal thickness enabled the epoxide and secondary amine conversion to be measured directly from the calibration curve by measuring their respective areas after adjusting for the amount of epoxy resin present.

In order to measure the amount of side reactions occurring during cure or post-cure, the following equation was used:

$$\alpha_{\text{epoxide}} = \frac{\alpha_{\text{NH}} + 1}{2} \tag{1}$$

where α_{epoxide} and α_{NH} are the fractional conversions of the epoxide and secondary amines, respectively. This equation assumes that only epoxy/amine addition takes place, so it can be used to determine a theoretical or "calculated" epoxide conversion from the known secondary amine conversions. Any deviation of the experimental epoxide conversion from the calculated epoxide conversion would indicate the occurrence of side reactions.

2.5. Determination of density

Densities were measured using a Micromeritics pycnometer. Approximately 4 g of resin known to four decimal places were sealed in the pressure chamber prior to measurement. The pressure that the chamber reached during the fill and purge cycle was approximately 17.5 psi. The measured density was an average of 10 separate measurements.

2.6. Determination of water uptake

Water uptake was measured gravimetrically by drying samples in a circulating oven for 2 days to remove any residual moisture prior to testing. Five replicates of each sample (dimensions $10 \times 45 \times 1.6$ mm^3) were immersed in water at 80°C for a total of 14 days and the water uptake was measured by removing the samples at different times, removing surface moisture with tissue paper and then weighing them. This was done after 1, 2, 3, 4, 7, 9, 11 and 14 days immersion.

2.7. Measurement of fracture toughness

Fracture toughness testing was carried out using the compact tension method according to ASTM E-394-81 using an Instron 4486 universal tester. Prior to testing, the exact dimensions were measured and the specimens were precracked by inserting a thin razor blade into the machined notch and impacting with a hammer to give a natural crack. In order to prevent crack blunting, a fresh razor blade was used for each specimen. The specimens were then placed into a jig and tested at a crosshead speed of 1.3 mm/min. After fracture, the exact crack length was measured from the fracture surfaces using an optical microscope fitted with a ruler. The fracture toughness at crack initiation, in terms of the critical stress intensity factor, K_{1C}, was calculated according to the following equation:

$$K_{1C} = \frac{PY}{BW^{1/2}} \tag{2}$$

where P is the maximum load obtained from the fracture load–deflection curve, B and W are the thickness and width

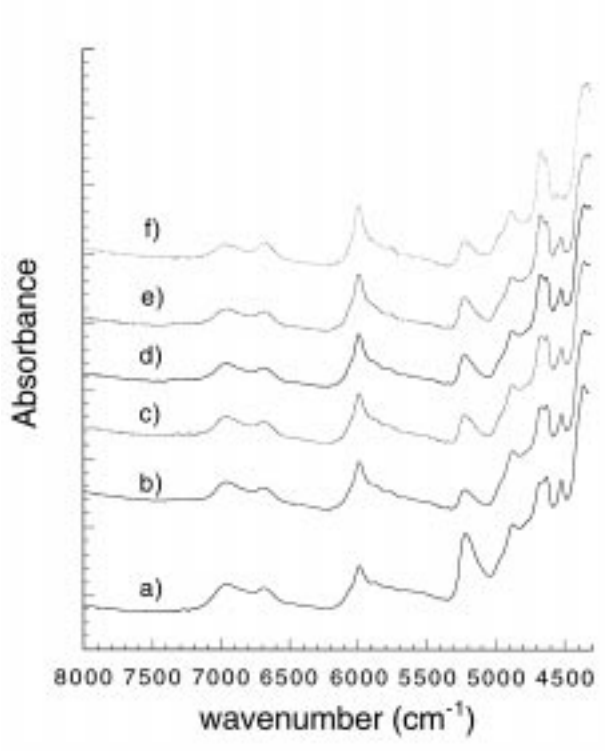

Fig. 3. Selection of near infra-red spectra of samples at varying PSF content after cure at 150°C. Also shown is a 30% w/w PSF sample that had been prereacted with TGAP in the presence of TMAH.

of the specimen, respectively, and Y is expressed as follows

$$Y = f(R) = \frac{(2+R)(-0.886 + 4.64R - 13.32R^2 + 14.72R^3 - 5.6R^4)}{(1-R)^{3/2}} \quad (3)$$

where $R = a/W$ and a is the crack length. A minimum of five specimens were used to determine the final K_{1C} for each test.

2.8. Measurement of compressive properties

Compressive tests were also performed using the Instron 4486 universal tester according to ASTM method D695-80. Prisms of dimensions $40 \times 10 \times 10$ mm^3 were machined and placed between horizontal platens with the crosshead speed in each case being 1.3 mm/min in the downward direction. The compressive modulus, yield stress and compressive strength were all determined from this test using a minimum of six replicates.

3. Results and discussion

3.1. Near infra-red spectroscopy

A selection of NIR spectra is shown in Fig. 3, which shows clearly the epoxide peaks at 4522 cm^{-1} and the secondary amine peaks at 6577–6692 cm^{-1} that were used here to quantify the epoxide and secondary amine conversions.

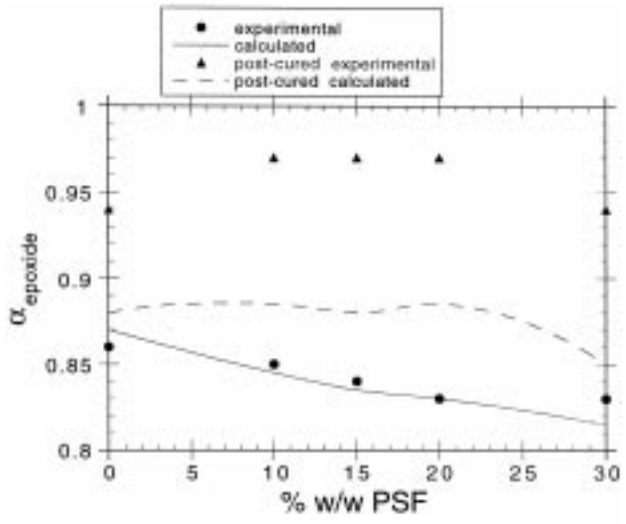

Fig. 4. Plot of the calculated and experimental epoxide conversions after cure and post-cure for the non-prereacted samples versus PSF content.

The addition of PSF has previously been shown to cause the epoxide conversion of the cured TGAP/DDS network [24] to decrease. It is of great interest however, to find out how, both the epoxide *and* secondary amine conversions are affected by PSF addition and whether this leads to an increase in side reactions such as etherification. The amount of side reaction, such as etherification occurring was determined from Eq. (1) using the theoretical epoxide conversion and comparing it to the experimental epoxide conversion. Fig. 4 shows that the experimental and calculated epoxide conversions after cure are very similar to each other, regardless of PSF concentration, which tends to indicate that increasing PSF concentration does not promote the etherification reaction in this case. Also shown in Fig. 4 are the calculated and experimental epoxide conversions after post-cure, which show that calculated epoxide conversion is well below the experimental epoxide conversion. This indicates that side reactions occurred to a far greater extent during post-cure. Again, however, it appeared that the amount of PSF did not affect the degree of etherification.

The calculated and experimental epoxide conversions determined for the prereacted PSF modified samples are shown in Fig. 5. In contrast with the non-prereacted samples, the prereacted epoxide conversions *increased* with increasing PSF concentration even though the calculated epoxide conversion decreased. This means that epoxide groups were consumed in reactions that did not involve amine groups. This leads to the conclusion that more side reactions such as etherification are occurring with increasing PSF content. The same plot for the post-cured prereacted samples (Fig. 5) shows similar behaviour to the cured sample. Here the calculated and experimental epoxide conversions both exhibit a modest increase as expected after

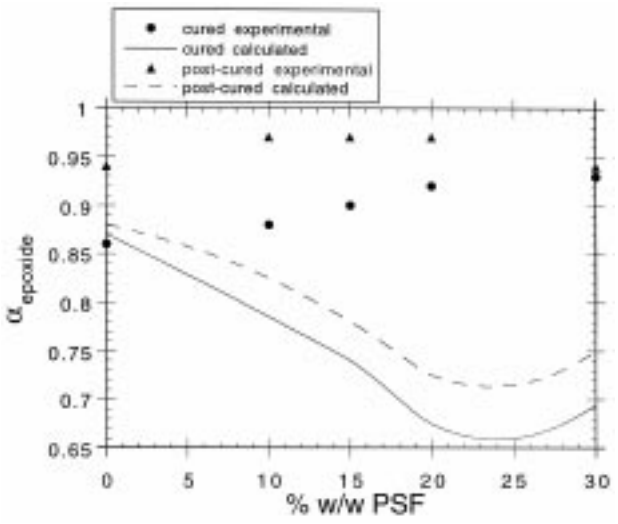

Fig. 5. Plot of the calculated and experimental epoxide conversions after cure and post-cure for the prereacted samples versus PSF content.

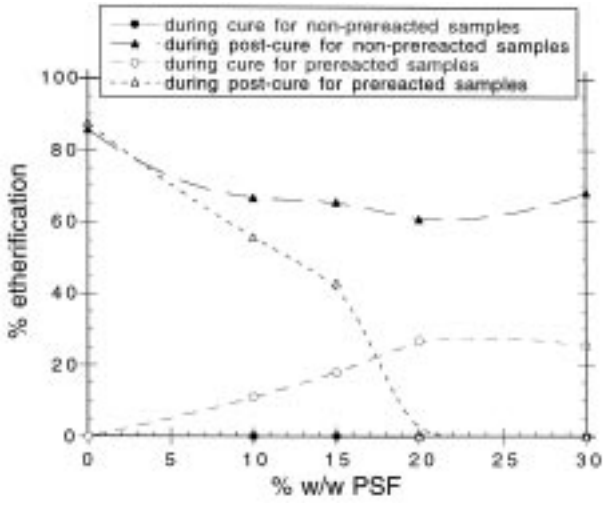

Fig. 6. Plot showing the amount of etherification occurring during cure and post-cure for the prereacted and non-prereacted samples versus PSF concentration.

further curing, but again the calculated epoxide conversion fell well below the experimental epoxide conversion, again indicative of side reactions

By comparing the experimental and the calculated epoxide conversion, the relative amounts of reaction occurring via secondary amine addition and etherification during both cure and post-cure were plotted in Fig. 6. Here it is clearly apparent that during cure, all of the reaction for the non-prereacted sample took place via epoxy/amine addition reactions with no etherification occurring. After post-cure, however, the situation is altered dramatically where it can be seen that around 70% of the reaction occurred via etherification. It is again interesting to note that increasing PSF content did not increase the amount of etherification occurring. This result is in contrast with results obtained by Min et al. [25] who showed (using a DGEBA/DDS system toughened with a PSF of molecular weight 10,000) that the amount of side reactions increased with increasing PSF concentration.

For the corresponding prereacted samples, the amount of etherification occurring during cure increased with increasing PSF, but in fact decreased during post-cure. This was likely to be caused by the increased concentration of amine groups available after cure which were not consumed during the cure, due to the increased etherification. These amine groups were then able to compete more equally with the etherification reaction that occurred during post-cure.

The amount of secondary amine addition or etherification occurring during both cure and post-cure for the prereacted and non-prereacted samples is shown in Tables 1 and 2, respectively. Both tables show that the amount of reaction occurring during post-cure is small in comparison to the initial cure, as would be expected. They also show that as a result of post-cure, the epoxide conversion for the non-prereacted samples increased by an average of 12%, while the average epoxide conversion for the prereacted samples increased by only 7.3%. This is a consequence of the prereacted samples achieving a higher epoxide conversion, thus reducing the amount of reaction that can occur subsequently during post-cure.

Table 1
Fractional conversions of the amine (α_{amine}) and etherification (α_{ether}) reactions for the non-prereacted samples as a result of cure and post-cure

% w/w PSF	After cure			As a result of post-cure		
	α_{amine}	α_{ether}	α_{total}	α_{amine}	α_{ether}	α_{total}
0	0.87	0.00	0.87	0.01	0.07	0.08
10	0.85	0.00	0.85	0.04	0.08	0.12
15	0.84	0.00	0.84	0.045	0.085	0.13
20	0.83	0.00	0.83	0.055	0.085	0.14
30	0.82	0.01	0.83	0.035	0.075	0.11
					Average	0.12

3.2. Dynamic mechanical thermal analysis

Dynamic mechanical thermal analysis was performed on the PSF modified samples in order to further investigate the behaviour of PSF and TGAP in each of the separate phases. The tan δ and bending modulus spectra obtained from a dynamic scan of the cured samples are shown in Fig. 7(a) and (b). As can be seen from each of the spectra, the resin system displays three transitions, manifesting themselves as peaks in the tan δ spectra and sharp drops in modulus in the bending modulus spectra. The first transition, denoted $^{PSF}T_g$, is the T_g associated with the PSF rich phase while the second and third are associated with different T_gs of the cured network. The second transition is referred to as $^{\alpha}T_g$, and is the T_g associated with a thermosetting system usually found approximately 10–30°C above the cure temperature. The

Table 2
Fractional conversions of the amine (α_{amine}) and etherification (α_{ether}) reactions for the prereacted samples as a result of cure and post-cure

PSF	After cure			As a result of post-cure		
	α_{amine}	α_{ether}	α_{total}	α_{amine}	α_{ether}	α_{total}
0	0.87	0.00	0.87	0.01	0.07	0.080
10	0.785	0.095	0.88	0.04	0.05	0.090
15	0.74	0.16	0.90	0.04	0.03	0.070
20	0.675	0.245	0.92	0.05	0.00	0.050
30	0.695	0.235	0.93	0.055	0.00	0.055
					Average	0.073

third transition is denoted ${}^{u}T_g$ and corresponds to the maximum T_g possible for the TGAP/DDS at a particular cure temperature. The appearance of the two transitions related to the epoxy network, while not common, has been reported previously for epoxy resins possessing high functionality. It was observed for a tetra-functional TGDDM/DDS resin system by Keenan et al. [26] at lower levels of DDS and was attributed to further curing of unreacted species in the rubbery state.

In another publication [24] it has been shown that the 10 and 15% PSF samples display a dispersed particulate morphology, the 20% displays a co-continuous morphology and the 30% PSF sample displays a phase inverted morphology. The tan δ and bending spectra shown here are clearly very sensitive towards these changes in morphologies. The size of the tan δ peaks and the magnitude of the drop in modulus for the PSF phase also exhibit three distinct environments which would correlate with a disperse, co-continuous and phase inverted morphology. Fig. 8(a) and (b) shows the corresponding tan δ and bending modulus spectra after post-cure where it can be seen that the α transitions

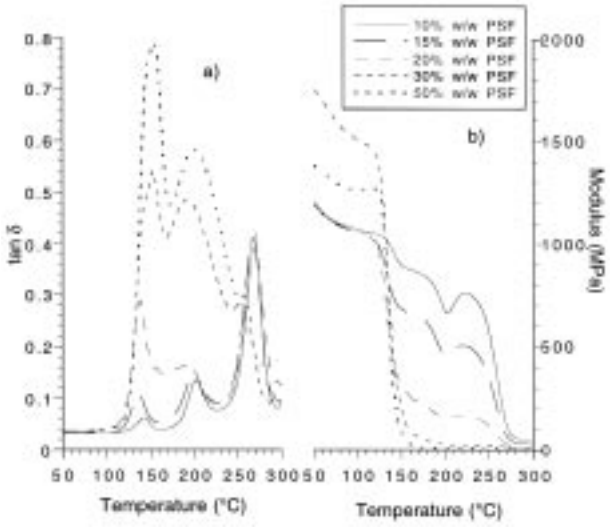

Fig. 7. Experimental (a) tan δ, and (b) bending modulus spectra of the cure PSF modified TGAP/DDS blends.

disappear completely for the samples at lower PSF concentration but remain for the higher concentration samples. Senich et al. [27] observed a similar phenomenon for a TGDDM/DDS system and attributed it to the coherence of the network and the decreasing number of reactive sites available with increasing conversion. Clearly then, when the morphology is made up of PSF particles dispersed within the epoxy continuous matrix (10 and 15% PSF), post-curing at higher temperatures enables the unreacted epoxy species to be consumed. However, when the morphology is more complex, either co-continuous or phase inverted, further reaction of the epoxy amine species is inhibited, a result of the expected increased miscibility of epoxy resin in the thermoplastic phase.

Fig. 9 plots the ${}^{u}T_g$ versus PSF concentration for the prereacted and non-prereacted samples after both cure and post-cure. The ${}^{u}T_g$ for the non-prereacted samples is largely unaffected by PSF concentration up to 20% PSF, after which there is a significant decrease. This decrease in ${}^{u}T_g$ at higher thermoplastic concentrations has been reported in similar studies by Cho et al. *[7]* and MacKinnon et al. *[28]*. Cho et al. attributed the decrease in ${}^{u}T_g$ to either an increase in miscibility of the thermoplastic or an increased solubility of the epoxy or hardener in the thermoplastic phase resulting in a looser network. MacKinnon et al., however, explained the decrease in terms of the increasing free volume of the network resulting from the addition of thermoplastic.

Also shown in Fig. 9 is the ${}^{u}T_g$ of the prereacted samples which exhibited a much larger decrease in ${}^{u}T_g$ with increasing PSF content. This decrease in ${}^{u}T_g$ is likely to be a result of the increased amount of etherification occurring as shown by NIR measurements. Etherification would reduce the T_g of the system in two ways, through the greater flexibility of the ether linkage plus the reduced crosslink density caused by internal cyclisation [29]. Internal cyclisation would be expected to be particularly favourable due to the greater ease with which it takes place in the glassy state. Post-curing both the prereacted and non-prereacted samples, however, was found to have little effect on the ${}^{u}T_g$s.

Fig. 10 plots the behaviour of ${}^{PSF}T_g$ after cure and post-cure for both the prereacted and non-prereacted samples. As can be seen, all of the samples display an initial decrease in ${}^{PSF}T_g$ up to 15% PSF followed by an increase. The changes bear a striking resemblance to a binodal phase diagram curve and can be used here to explain the observed results. The 15% PSF, being the sample closest to the critical volume fraction would be expected to phase separate first, when the epoxy amine molecules are at their smallest (i.e. cure conversion is at its lowest). This may then facilitate the trapping of a larger amount of epoxy/amine molecules in the PSF phase prior to any increase in viscosity, thus producing the largest depression in ${}^{PSF}T_g$. At other compositions, the molecular weight of the resin species would be higher at the point of phase separation, thereby decreasing the amount of epoxy/amine molecules that get trapped in the PSF phase, thus causing a smaller depression in ${}^{PSF}T_g$. The prereacted

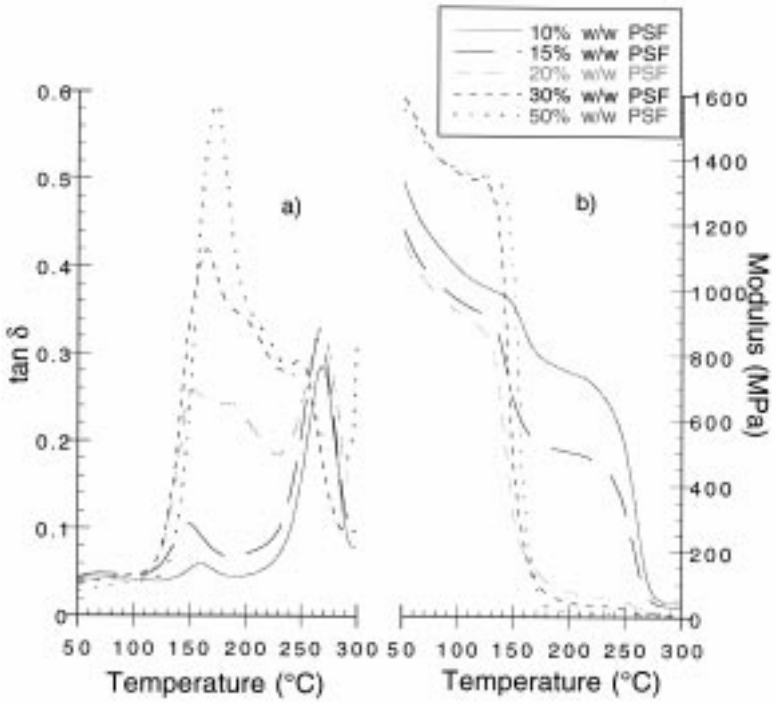

Fig. 8. Experimental (a) tan δ, and (b) bending modulus spectra of the post-cured PSF modified TGAP/DDS blends.

samples show a similar behaviour but the higher $^{PSF}T_g$s at higher PSF concentrations suggest that the greater epoxy cure conversion and increased etherification produces a much greater degree of phase separation of the epoxy amine from the continuous PSF phase. The $^{PSF}T_g$s after post-cure for both the prereacted and non-prereacted samples exhibit a consistent increase over the entire concentration range indicating that a comparatively similar amount of epoxy amine is expelled from the respective PSF phases. Clearly, post-curing the system imparts greater mobility to all the species equally, allowing further phase separation to occur and increasing the T_g of the PSF phase.

3.3. Density

The density of the prereacted and non-prereacted PSF modified samples after post-cure only is shown in Fig. 11. It can be clearly seen that the density decreases with increasing PSF content and appears not to be affected by prereaction. The decrease in density appears to be simply a reflection of the fact that PSF is less dense than the cured epoxy/amine matrix. The interfacial regions would also be expected to result in a decrease in density with increasing PSF concentration. Interestingly, there appears to be no effect of morphology on the density. The main conclusion

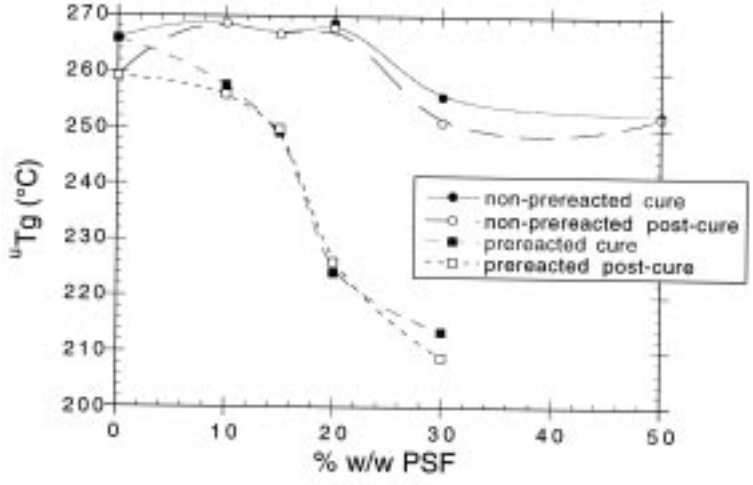

Fig. 9. Plot of $^{u}T_g$ versus PSF concentration for the prereacted and non-prereacted samples after cure and post-cure.

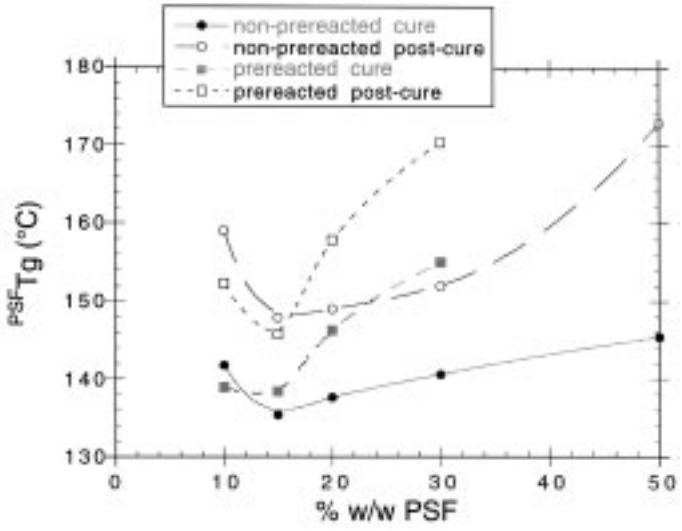

Fig. 10. Plot of $^{PSF}T_g$ versus PSF concentration for the prereacted and non-prereacted samples after cure and post-cure.

drawn from the result is that the etherification reaction does not affect the molecular packing of the network.

3.4. Water uptake

The water uptake of the prereacted and non-prereacted samples after cure and post-cure was measured for samples immersed in water at 80°C over a period of 14 days. Fig. 12 shows that for each PSF concentration, the water uptake was rapid in the early stages, but gradually levelled off, even though after 14 days at 80°C the absorption of water still had not ceased completely. The percentage of water uptake obtained after the 14-day period were plotted versus PSF content and are shown in Fig. 13. The results show that all of the samples displayed an overall decrease in water uptake with increasing PSF concentration, albeit in an irregular fashion. The shape of the water uptake plots highlights the complexity of the various contributions that determine moisture ingress, such as polarity, free volume and morphology. The biggest factor causing the overall decrease in water uptake is the decreasing polarity of the resin mixture as the amount of PSF was increased. The PSF molecule is much less polar than the epoxy network and is thus more resistant to moisture ingress. However, the behaviour is more complicated because superimposed upon the overall decrease is a modest increase in water uptake for the 10 and 15% PSF samples. This may be a result of the interfacial regions in a particulate morphology being more susceptible to moisture ingress than a co-continuous structure. The prereacted samples were found to exhibit slightly greater water uptake after cure than were the non-prereacted samples. This is likely to be a result of the increased amount of unreacted amine groups present in the continuous epoxy phase providing sites for hydrogen bonding as a result of the increase in etherification. After post-cure, however, the water uptake for the non-prereacted samples was

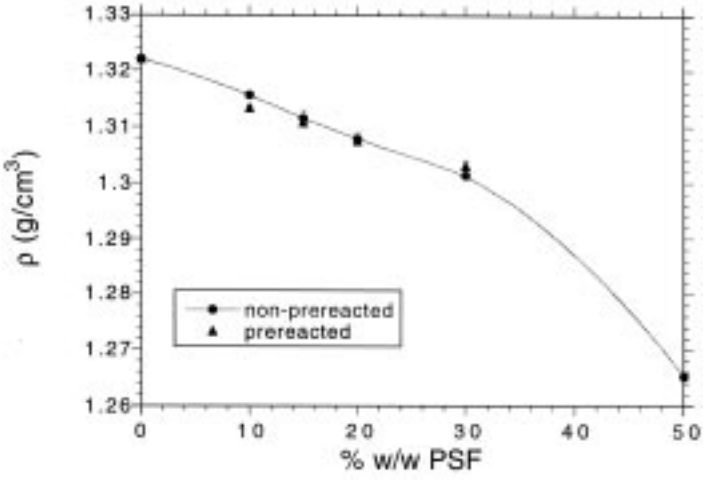

Fig. 11. Plot of density versus PSF concentration for the prereacted and non-prereacted samples after post-cure.

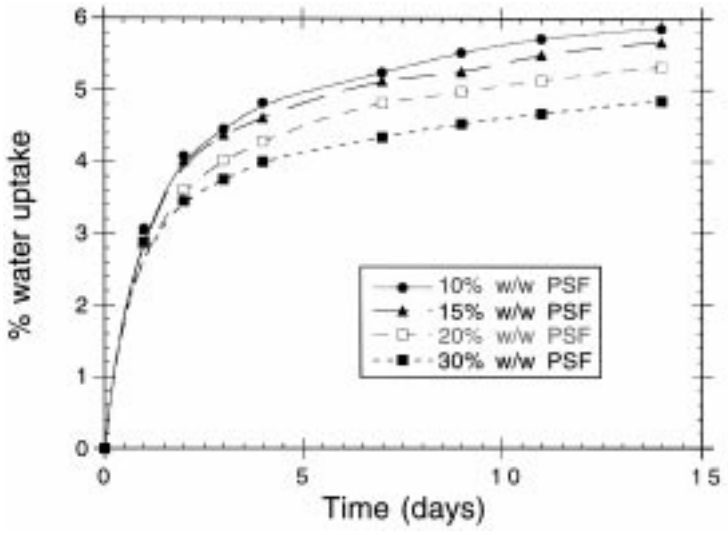

Fig. 12. Plot of the percentage of water uptake with time for the 10, 15, 20 and 30% w/w PSF modified samples after cure.

significantly higher than for the post-cured prereacted samples. The much smaller difference between the water uptake of the prereacted and non-prereacted samples may well be a result of an increase in interaction between the PSF and epoxy phases caused by prereaction.

3.5. Fracture toughness

The toughness of the post-cured PSF modified TGAP/DDS samples, both prereacted and non-prereacted, was measured on an Instron Testing Machine using the compact tension method according to ASTM E-399-81. Fig. 14 plots K_{1C}, the stress intensity factor, versus PSF concentration where it is apparent that the toughness of the highly cross-linked TGAP/DDS system increased with increasing PSF concentration. The K_{1C} increased modestly at the lower PSF concentrations, but increased more dramatically for the 20% PSF sample. By comparing these results with the changes in morphology (previously reported [24]) it is evident that this corresponds to the initial formation of a co-continuous or phase inverted structure. This result supports many studies reported in the literature [5–7] and demonstrates the necessity of a material having a complex morphology in order to achieve good toughness enhancement when a thermoplastic is used.

The K_{1C} of the prereacted PSF samples in Fig. 14 show that toughness was not enhanced by prereaction, but was in fact reduced. The reason for this may be that prereaction, while increasing the adhesion of the PSF phase to the epoxy phase, increases the amount of etherification, which in this case appears to decrease the toughness of the cured network.

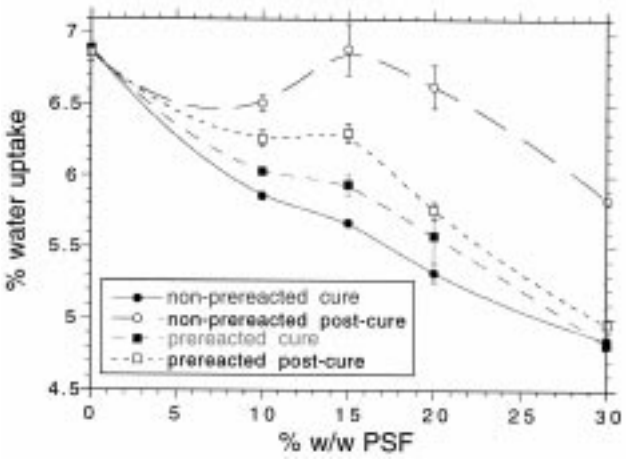

Fig. 13. Plot of the percentage of water uptake after 14 days immersion in water at 80°C for the prereacted and non-prereacted samples after cure and post-cure versus PSF concentration.

3.6. Compressive properties

The compressive modulus was determined according to the ASTM-D695-80 standard for the post-cured prereacted and non-prereacted samples. The great advantage that thermoplastic toughening has over the use of rubbers as toughening additives (and the driving force behind its use), is that it does not reduce other desirable properties of the epoxy matrix, such as the modulus, and yet still achieves good toughness enhancement. This was borne out in the results here as shown in Fig. 15 where the non-prereacted modulus was relatively unaffected by PSF addition. The modulus of the prereacted samples was marginally lower than the non-prereacted samples but showed little dependence upon PSF concentration.

The yield stress and compressive strength were found to decrease with increasing PSF content as shown in Figs. 16 and 17, respectively. The yield stress, a small strain property [30] would be expected to decrease as a result of the decreasing density of the system and the lower yield stress of the

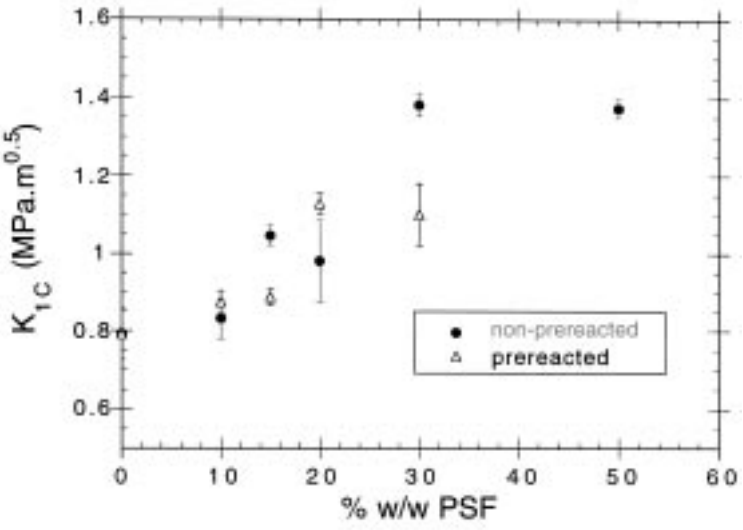

Fig. 14. Plot of the fracture toughness for the prereacted and non-prereacted samples after post-cure versus PSF concentration.

thermoplastic, as PSF is added. Conversely, the compressive strength, a large strain property, dependent upon long range motions which are affected by crosslink density would also be expected to decrease, but more as a result of the decreasing crosslink density of the system as PSF is added. Clearly then, the decreases observed for both of these properties would be expected with the addition of a less dense linear thermoplastic polymer with a lower yield stress.

4. Summary

This work has shown how PSF addition affects the chemical structure, mechanical and physical properties of the cured and post-cured TGAP/DDS network for the prereacted and non-prereacted samples.

1. Near infra-red spectroscopy showed that during cure of the non-prereacted samples, all of the reaction occurred via epoxide/amine addition reactions, while during post-cure, most of the reaction takes place via etherification. For the prereacted samples, the amount of etherification that occurred increased with increasing PSF content during cure. This consequently resulted in a large increase in the amount of secondary amine addition occurring during post-cure.
2. DMTA was able to predict the type of morphology present, which correlated well with transmission electron

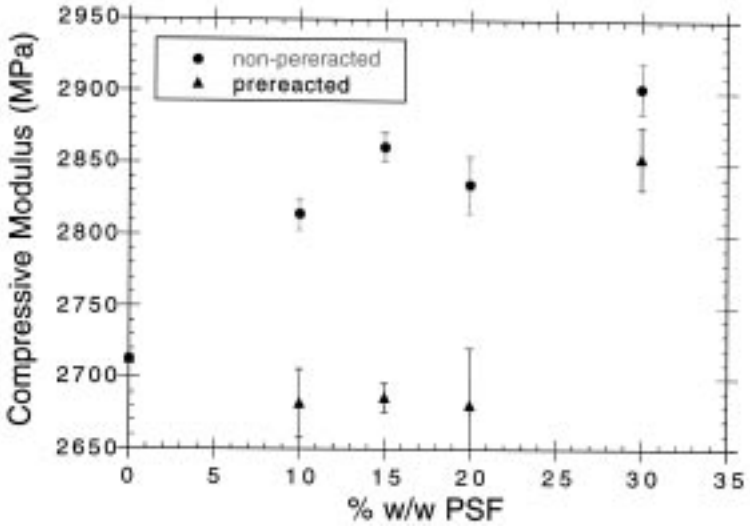

Fig. 15. Plot of the compressive modulus of the prereacted and non-prereacted samples after post-cure versus PSF concentration.

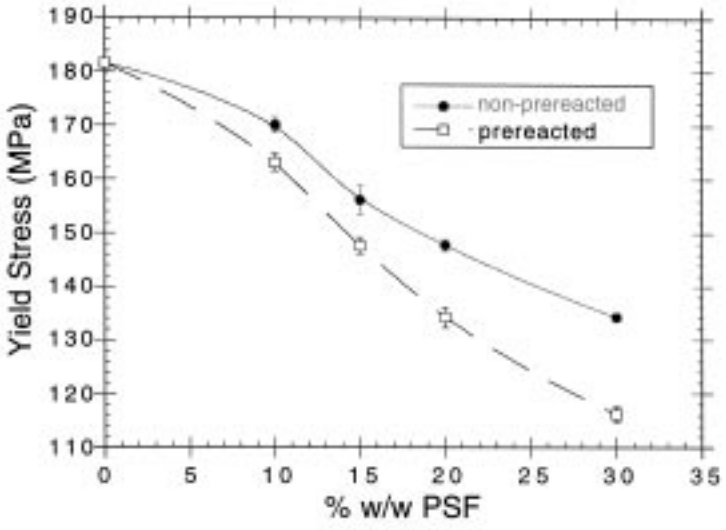

Fig. 16. Plot of the yield stress of the prereacted and non-prereacted samples after post-cure versus PSF concentration.

micrographs. It also showed that there was considerable miscibility of TGAP in the PSF phase, but comparatively little PSF miscibility in the TGAP phase. The ${}^{u}T_{g}$s for the non-prereacted samples, however, exhibited little dependence upon the changing miscibilities, but decreased sharply when the morphology changed to a phase inverted structure. The prereacted samples exhibited a much larger decrease in ${}^{u}T_{g}$ corresponding to an increased amount of etherification.

3. The changes in ${}^{PSF}T_{g}$ highlighted the miscibility and phase separation process of the TGAP in the PSF phase. The miscibility of TGAP in the PSF phase was shown to have a dominant effect on the changes in ${}^{PSF}T_{g}$ when the morphology was particulate in nature. However, when the morphology became co-continuous, TGAP was able to phase separate from the continuous PSF phase, thereby increasing ${}^{PSF}T_{g}$. Prereaction supported this conclusion by showing further increases in ${}^{PSF}T_{g}$ caused by further phase separation as a result of an increase in epoxide cure conversion.
4. Physical properties such as density, free volume and water uptake were also measured for the cured samples. The density was unaffected by prereaction but decreased with increasing PSF content. The water uptake, however, exhibited more complex behaviour and was found to be sensitive to polarity, free volume, and the interaction of the phases.
5. The toughness of the system was found to be dependent upon morphology, with relatively small increases in toughness observed when the morphology remained dispersed particulate or co-continuous in nature. A much larger increase in toughness was found when the

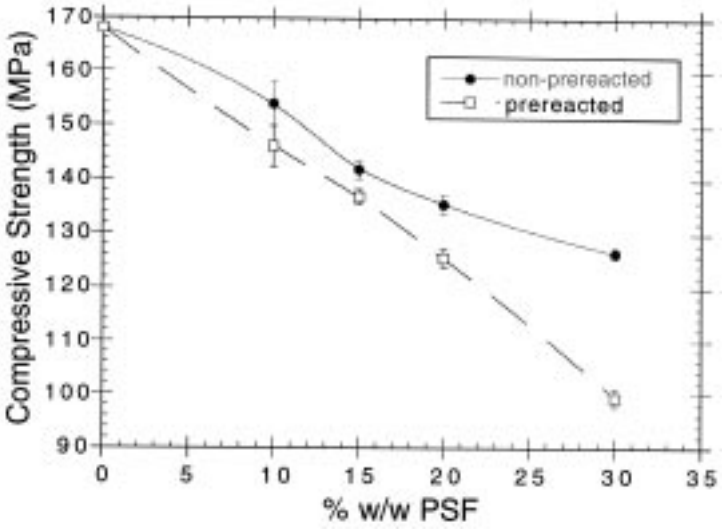

Fig. 17. Plot of the compressive strength of the prereacted and non-prereacted samples after post-cure versus PSF concentration.

morphology became phase inverted. The prereacted samples, however, failed to improve the toughness of the systems, indicating that etherification was not beneficial to improving mechanical properties. The modulus was found to be relatively unaffected regardless of whether the samples were prereacted or non-prereacted, justifying one of the main practical reasons for using thermoplastics as tougheners. Mechanical properties such as yield stress and compressive strength were found to be dependent upon small and large strain properties, respectively, as would be expected, but also showed that they were adversely affected by etherification.

References

[1] Sankaran S, Chanda M. J Appl Polym Sci 1990;39:1635.
[2] Bucknall CB, Partridge IK. Br Polym J 1983;15:71.
[3] Bucknall CB, Partridge IK. Polymer 1983;24:639.
[4] Raghava RS. 28th National SAMPE Symposium, 1983. p. 367.
[5] Recker HG, Allspach T, Altstadt V, Folda T, Heckmann W, Itteman P, Tesch H, Weber T. SAMPE Quarterly 1985;21:46.
[6] MacKinnon AJ, Jenkins SD, McGrail PT, Pethrick RA. Macromolecules 1992;25:3492.
[7] Cho JB, Hwang JW, Cho K, An JH, Park CE. Polymer 1993;34:4832.
[8] Li SJ, Hsu B-L, Harris FW, Cheng SZD. Polym Prepr (Am Chem Soc, Div Polym Chem) 1994:51.
[9] Street AC, McGrail PT. Proceedings of Compalloy Europe, 1991. p. 145.
[10] Fu Z, Sun Y. Polym Prepr (Am Chem Soc, Div Polym Chem) 1988;29:177.
[11] MacKinnon AJ, Jenkins SD, McGrail PT, Pethrick RA. J Appl Polym Sci 1995;58:2345.
[12] Yoon TH, Liptak SC, Priddy DB, McGrath JE. J Adhesion 1994;45:191.
[13] Hay JN, Woodfine B, Davies M. High Perf Polym 1996;8:35.
[14] Stangle M, Altstadt V, Tesch H, Weber Th. Adv Mater: Cost Eff, Qual Cont, Health Environ 1991:33.
[15] Hedrick JL, Yilgor I, Wilkes GL, McGrath JE. Polym Bull 1985;13:201.
[16] Murakami A, Ioku T, Saunders D, Aoki H, Yoshiki T, Murakami S, Watanabe O, Saito M, Inoue H. Proceedings of the Benibana International Symposium of Polymer Toughening, 1990. p. 65.
[17] Recker HG, Allspach T, Altstadt V, Folda T, Heckmann W, Itteman P, Tesch H, Weber T. 34th International SAMPE Symposium, 8–11 May 1989. p. 747.
[18] Recker HG, Altstadt V, Eberle W, Folda T, Gerth D, Heckmann W, Itteman P, Tesch H, Weber T. 21st International SAMPE Technical Conference, 25–28 September 1989. p. 283.
[19] Min BG, Hodgkin JH, Stachurski ZH. J Appl Polym Sci 1993;48:1303.
[20] Bell JP. J Appl Polym Sci 1970;14:1901.
[21] Johnson RN, Farnham AG, Clendinning RA, Hale WF, Merriam CN. J Polym Sci Part A-1 1967;5:2375.
[22] Varley RJ, Heath GR, Hawthorne DG, Hodgkin JH, Simon GP. Polymer 1995;36:1347.
[23] Varley RJ, Hawthorne DG, Hodgkin JH, Simon GP. J Appl Polym Sci 2000;77:237.
[24] Varley RJ, Hawthorne DG, McCulloch D, Hodgkin JH, Simon GP. Polymer 2000;41:3425.
[25] Min BG, Stachurski ZH, Hodgkin JH, Heath GR. Polymer 1993;34:3620.
[26] Keenan JD, Seferis JC, Quinlivan JT. J Appl Polym Sci 1979;24:2375.
[27] Senich GA, MacKnight WJ, Schneider NS. Polym Eng Sci 1979;19:313.
[28] MacKinnon AJ, Pethrik RA, Jenkins SD, McGrail PT. Macromolecules 1994;35:5319.
[29] Attias AJ, Bloch B, Laupretre F. J Polym Sci Part A: Polym Chem 1990;28:3445.
[30] Madsen PA, Foister RT. J Appl Polym Sci 1989;37:1931.